Two-phase flow metering of maldistribution inside a header by means of venturi flowmeter solely

Lecardonnel, A.; De Servi, C.; Colonna, P.; Laboureur, D.

DOI
10.1615/MultScienTechn.2023048066

Publication date
2024

Published in
Multiphase Science and Technology

Citation (APA)
Lecardonnel, A., De Servi, C., Colonna, P., & Laboureur, D. (2024). Two-phase flow metering of maldistribution inside a header by means of venturi flowmeter solely. *Multiphase Science and Technology*, *36*(1), 97-114. https://doi.org/10.1615/MultScienTechn.2023048066

Multiphase Science and Technology, 36(1):97–114 (2024)

TWO-PHASE FLOW METERING OF MALDISTRIBUTION INSIDE A HEADER BY MEANS OF VENTURI FLOWMETER SOLELY

A. Lecardonnel,[1,2,*] C. De Servi,[2] P. Colonna,[2] & D. Laboureur[1]

[1]*Von Karman Institute for Fluid Dynamics, Rhode-St-Genese, Belgium, B-1640*

[2]*Delft University of Technology, Delft, Netherlands*

*Address all correspondence to: A. Lecardonnel, Von Karman Institute for Fluid Dynamics, Rhode-St-Genese, Belgium, B-1640, E-mail: aude.lecardonnel@vki.ac.be

Original Manuscript Submitted: 3/6/2023; Final Draft Received: 8/17/2023

In evaporators, the distribution of the liquid and vapor phases among the channels is a convoluted problem, depending on a wide range of parameters. However, maldistribution causes important losses of performance. Due to their complexity, the accurate modeling of such two-phase flows is difficult to handle. Hence, experimental studies are still of great importance to help the understanding of maldistribution behaviors inside evaporators. Most of the experimental investigations of two-phase flow distribution are measuring the liquid and vapor quantities in the channels through a phase separation process, increasing the test duration and complexity. As a consequence, the number of parameters investigated is usually limited. Therefore, a new inline instrumentation method would allow for a more complete study by simplifying the measurement process. In the present work, an isothermal air/water mixture was used as fluid. The distribution of the two phases in eight channels of 10-mm I.D. connected to a simplified header was investigated. The inlet mass flow rates considered ranged from 0 to 0.025 kg/s for the water, and from 0 to 0.022 kg/s for the air. Consequently, qualities x up to 0.7 and void fractions α up to 0.9 were reached. All the tests were carried at a pressure condition of 7 bar to reach a liquid to vapor density ratio similar to what is encountered for traditional refrigerant. Finally, to allow a continuous measurement process, the mass flow rates in each of the 10-mm I.D. channel were measured using a flowmeter calibrated on a separate line. Since no void fraction meter was coupled, a new iterative methodology, based on the Venturi pressure drops measurement solely, was developed and is proposed here. It proved to successfully predict the vapor and liquid phase flow rates in each channel.

KEY WORDS: *liquid-gas two-phase flow, experimental, metering instrumentation, Venturi, heat exchanger, evaporators, maldistribution*

1. INTRODUCTION

Evaporators are usually multiple parallel channels heat exchangers that are encountered in various industrial applications, the most common ones being vapor cycle systems for air conditioning. At the inlet of an evaporator, the refrigerant can be found in its liquid phase, or as a liquid/vapor mixture. Due to the presence of this two-phase flow, the uniformity of the distribution among the channels is hard to predict. Unfortunately, nonuniform distribution in an evaporator header leads to a lower efficiency (Choi et al., 2003). The liquid phase distribution is especially the most critical criterion. Besides, the homogeneity of the distribution depends on

many parameters with a varying range of impacts. Many studies intended to assess their effects, and were listed by several reviews (Dario et al., 2013; Leblay, 2012). The main parameters of influence have been gathered from Dario et al. (2013) and consist in [note—no colon]: liquid and vapor flow rates (thus flow pattern), header and channels orientation, presence of a diffuser device, tube intrusion, and inlet tube position and diameter. However, each study focuses on a limited number of parameters, due to the complexity of the flow rate measurement process.

Traditionally, in two-phase flows studies, the mass flow rates of each phase is measured through phase separation at the outlet of each channel. However, phase separation is a time consuming and costly solution, especially when the number of channels and the number of tests to be performed are large. Besides, when several header and channel orientations have to be tested, a large test area is required and phase separation techniques do not provide enough flexibility. Therefore, in this study, the measurement of the two-phase flow in the channels will be performed using an inline instrumentation. Multiple solutions were investigated through a multiphase flow metering literature survey (Lecardonnel et al., 2021). Industrial flow meters exist for two-phase flows, such as Coriolis, true mass flow, and electromagnetic flow meters. Even though these instruments were considered, their great dimensions even for small pipe diameters made their implementation in the present setup complicated. Other studies have attempted to develop new innovative designs for multiphase flow meters (de Paula Pellegrini et al., 2017; Xie et al., 2007), but either their range of operating conditions application was too narrow or the development was at a too early stage. The solution chosen is based on Venturi flowmeters (VFM), which are low-cost, compact, inline, and promising instruments when it comes to liquid/gas or liquid/vapor flow measurements (Bertani et al., 2010). Very often, they are coupled to an upstream void fraction meter installed on the pipe (Meng et al., 2010; Oliveira et al., 2009). These void fraction meters are usually either intrusive, hard to implement on multiple parallel channels, or very costly. Besides, they are not yet commercially available. Thereby, the purpose of the article is to present a new inline measurement technique of a two-phase mass flow rate using a VFM solely. This work is part of a broader purpose which is to be able to perform a large parametric study of the features impacting a two-phase flow distribution inside a simplified evaporator. For the first time, after the introduction of the topic of this study, the principle of Venturi flow metering for two-phase flows is summarized. The calibration of the VFM used in the present study is then presented, as well as the proposed methodology. For a second time, the uncertainties related to these measurements are evaluated. Finally, the application of the measurement technique in a simplified isothermal evaporator is proposed as well as examples of measurements of good and bad flow distributions.

2. TWO-PHASE FLOW RATE MEASUREMENT WITH VENTURI

2.1 Theory

For a two-phase flow, the determination of the total mass flow rate $\dot{m}_{\text{TP}}$ by a VFM is achieved very similarly as for a single phase flow (Oliveira et al., 2009):

$$\dot{m}_{\text{TP}} = \sqrt{2}\frac{F_a Y C_{d,\text{TP}} A_{\text{throat}}}{\sqrt{1-\beta^4}}\sqrt{\rho_{\text{TP}}\Delta P_{\text{TP}}} = K_{\text{geo}} C_{d,\text{TP}}\sqrt{\rho_{\text{TP}}\Delta P_{\text{TP}}} \tag{1}$$

where TP refers to two-phase flow, F_a is the factor correcting for the thermal expansion, Y is the compressibility factor, $C_{d,\text{TP}}$ is the two phase discharge coefficient, A_{throat} is the throat cross-section in m^2, β is the throat to inlet diameter ratio, ρ is the density in kg/m^3, and ΔP_{TP} is the

differential pressure drop measured between the inlet and the throat sections of the VFM in Pa. This can be simplified by using $K_{\text{geo}} = \sqrt{2}.(F_a Y A_{\text{throat}}/\sqrt{1-\beta^4})$.

However, the evaluation of the two-phase density ρ_{TP} is not straightforward. The most common approach to simplify the determination of the two-phase mass flow $\dot{m}_{\text{TP}}$ is to replace the two-phase density ρ_{TP} and discharge coefficient $C_{d,\text{TP}}$ respectively by the liquid density ρ_l and the discharge coefficient determined for the liquid phase $C_{d,l}$. The two-phase flow condition is then taken into account through the use of a modeling coefficient K_l (Liu et al., 2020) which depends on the quality $x = \dot{m}_v/(\dot{m}_v + \dot{m}_l)$, where l refers to the liquid phase, being water in the present work, and v to the vapor phase, being air (Zhang et al., 1992).

$$\dot{m}_{\text{TP}} = K_{\text{geo}} C_{d,l} K_l \sqrt{\rho_l \Delta P_{\text{TP}}} \tag{2}$$

Thus, for a two-phase flow, another information besides the pressure drops is required, which generally is the quality x. As stated in Section 1, in almost every study, the VFM is coupled with an upstream void fraction meter installed on the pipe (Meng et al., 2010), usually a capacitance probe (Bertani et al., 2010; Oliveira et al., 2009; Zeghloul et al., 2021). The quality is indeed retrieved from the measured void fraction, either from an existing correlation or from a calibration. Once obtained, the quality together with the pressure drops from the VFM are used to calculate the total mass flow rate. However, capacitance sensors are still not yet easily commercially available and are only obtainable in a few research laboratories. Therefore, the development of a VFM that can be used without the information of the quality is greatly needed. To the authors' knowledge, only two studies so far attempted to tackle this issue: the research investigations from Shaban and Tavoularis (2014) and from Monni et al. (2014). The work from Shaban and Tavoularis (2014) relies on the use of machine learning techniques on differential pressure signals to retrieve the liquid and gas flow rates. To be able to use this work, the flow pattern needs to be identified and due to the pressure constraint in the current study (7 bar), this would be have been difficult to implement. Monni et al. makes also use of a VFM and exploits the irreversible pressure losses between the inlet and the outlet but only at very high void fraction and thus high quality. The method happens to be much more precise for the gaseous phase than for the liquid phase, which is the opposite of what is intented in the present work.

2.2 Calibration

The VFM is calibrated using an air/water mixture at 7 bar to obtain a density ratio between the two phases closer to the one typically encountered in refrigerants. Water is pumped from a tank by a centrifugal pump (Wilo Helix V 214-1/16/E/KS/400-50) and its flow rate is measured with an electromagnetic flowmeter (Fuji Electric ModMAG M1000). A 15 bar compressed air line is connected to the facility and its pressure is then decreased to around 6.5 barG through a pressure regulator. The air flow rate is measured thanks to a thermal mass flow sensor (CS Instruments VA 500). Air and water are then mixed together by means of an elbow pipe inserted in the main water pipe. The schematic of the test facility can be found in Fig. 1. The mixture is further sent to the test section. It can either be the simplified evaporator setup that will be presented in Section 4 or the calibration line. The latter consists simply in a flanged pipe of 10-mm I.D. on which a Venturi flow meter is welded. A straight pipe length of $50D$ is present ahead of the instrument to develop the flow (see Fig. 2), where D is the internal diameter of the flanged pipe. The orientation of the pipe can be vertical downward, vertical upward, or horizontal.

As explained in Section 1, VFM were selected to allow the measurement of the liquid and gas mass flows in a series of parallel tubes modeling the evaporator refrigerant channels. All

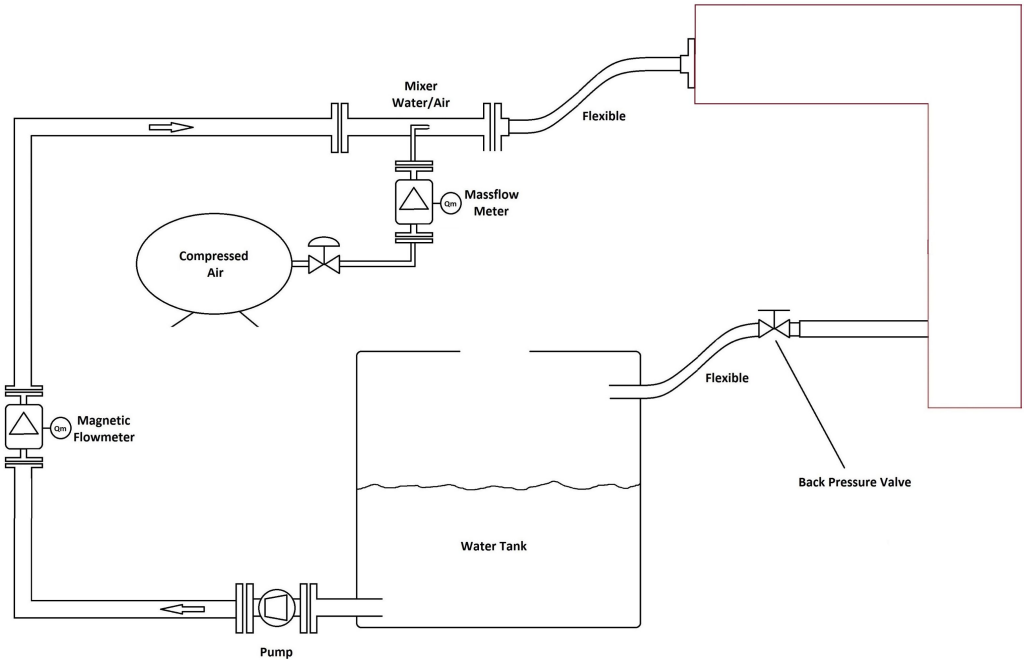

FIG. 1: Schematic of the test facility

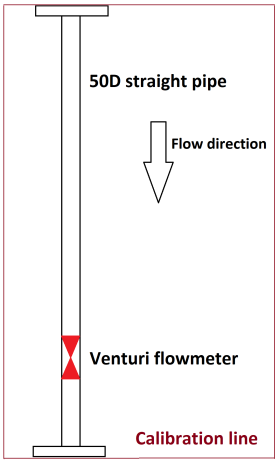

FIG. 2: Schematic of the calibration

the Venturi of the present study were designed at the Von Karman Institute (VKI), following the standard ISO 5167-4:2003 (2003) (see Fig. 3). However, this standard does not cover diameters smaller than 50 mm. The main recommendations in terms of pressure taps as well as upstream and downstream lengths were applied for the present design, and for the remaining dimensions, the proportions described in the document have been preserved. The four upstream pressure taps were interconnected in a triple-T arrangement as recommended in the ISO 5167-4:2003 (2003) and connected to one side of a differential pressure membrane sensor (Validyne DP15

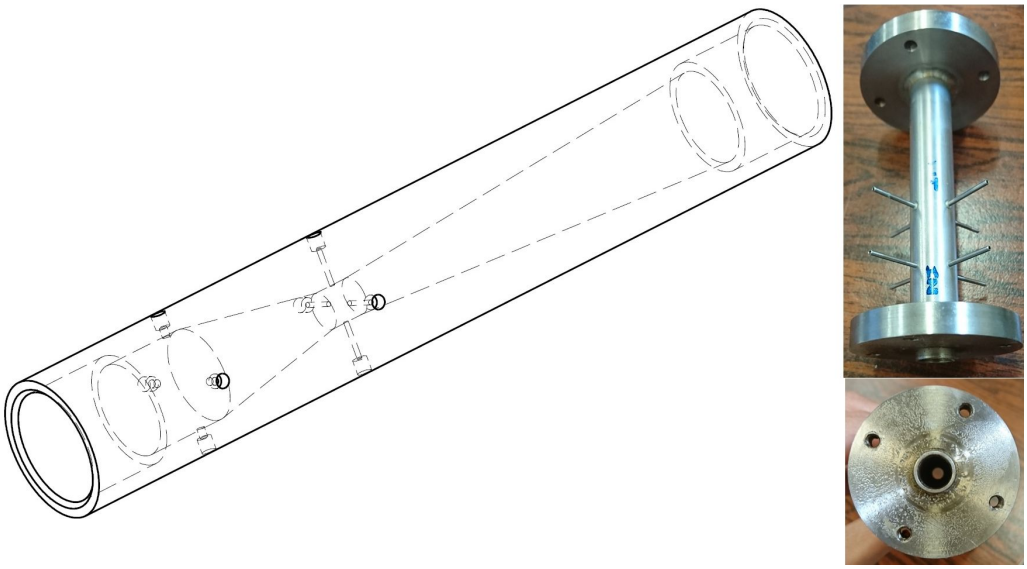

FIG. 3: Isometric view and picture of the Venturi

with a 750 mbar range). Similarly, the four throat pressure taps were also interconnected in a triple-T arrangement and connected to the other side of the sensor. The throat to inlet diameter ratio β of all the VFM used in the present study is equal to 0.42. This ratio was chosen to be low enough to create noticeable pressure drops even at small mass flow rates. The pressure difference measured by the membrane corresponds to the throat pressure drops ΔP_{TP} mentioned in Eq. (1). All these instruments were connected to a NI-DAQ (National Instrument) hardware, to acquire their signals at a frequency of 200 Hz and a duration of 90 s.

After the test section, the air/water mixture is again collected and sent back to the reservoir. A back pressure valve is present to set and control the targeted pressure.

2.3 Methodology

The proposed methodology to determine the total mass flow rate as well as the liquid and vapor flow rates solely with a VFM will be explained in this section. To begin with, since three unknowns in total are present in this system: $\dot{m}_v$, $\dot{m}_l$, and x, three equations are required. Several existing correlations relating two-phase flow specific numbers were tested, such as the two-phase flow multiplier Φ_l^2 (Baker, 2000) and the Lockhart–Martinelli parameter χ (Lockhart, 1949). The closure of the system was however not satisfying enough with these numbers. New possibilities were investigated by means of some ratio between the two-phase pressure drops across the Venturi ΔP_{TP} and the mass flow rates of the two phases $\dot{m}_{\text{air}}$ and $\dot{m}_{\text{water}}$ in the present document. Equations (3)–(5) present the three ratios that have been selected.

$$\frac{\dot{m}_{\text{water}}^2}{\Delta P_{\text{TP}}} = f(x) \tag{3}$$

$$\frac{\Delta P_{\text{TP}}}{\dot{m}_{\text{air}}} = g(x) \tag{4}$$

$$\frac{\Delta P_{\text{TP}}}{\dot{m}_{\text{air}} \times \dot{m}_{\text{water}}} = h(x) \tag{5}$$

The corresponding curves of these equations are shown in Fig. 4 below, for a vertical downward orientation of the Venturi. In the figures, both the experimental points and their mathematical fitting equations are displayed. All the experimental data presented in this section were obtained on the dedicated calibration line described in Section 2.2, for a single Venturi. It is recalled that the internal diameter of the pipe is 10 mm. The mass flow rates covered ranged from 0 to 0.025 kg/s for the water and from 0 to 0.022 kg/s for the air.

As one can see, when plotting the experimental points, strictly decreasing, very smooth, and continuous trends are obtained for $f(x)$, $g(x)$, and $h(x)$. Each curve can be accurately fitted by a sum of two exponential functions. The density was not considered in the equations, as it was kept constant during the tests and equal to 995 kg/m^3 for the water and to 7.8 $\pm$ 0.1 kg/m^3 for the air. The mathematical fittings of Eqs. (3)–(5) for the three orientations are displayed in Fig. 5. It has to be noted that experimental data for the vertical upward and horizontal orientations have also been collected but are not shown to improve the clarity of the figures.

It can be noticed from these figures that the orientation of the 10-mm I.D. pipe has a non-negligible effect on the curves, even though this impact is relatively low. Generally speaking, all the curves for the three orientations present similar curve shapes, with strictly decreasing trends.

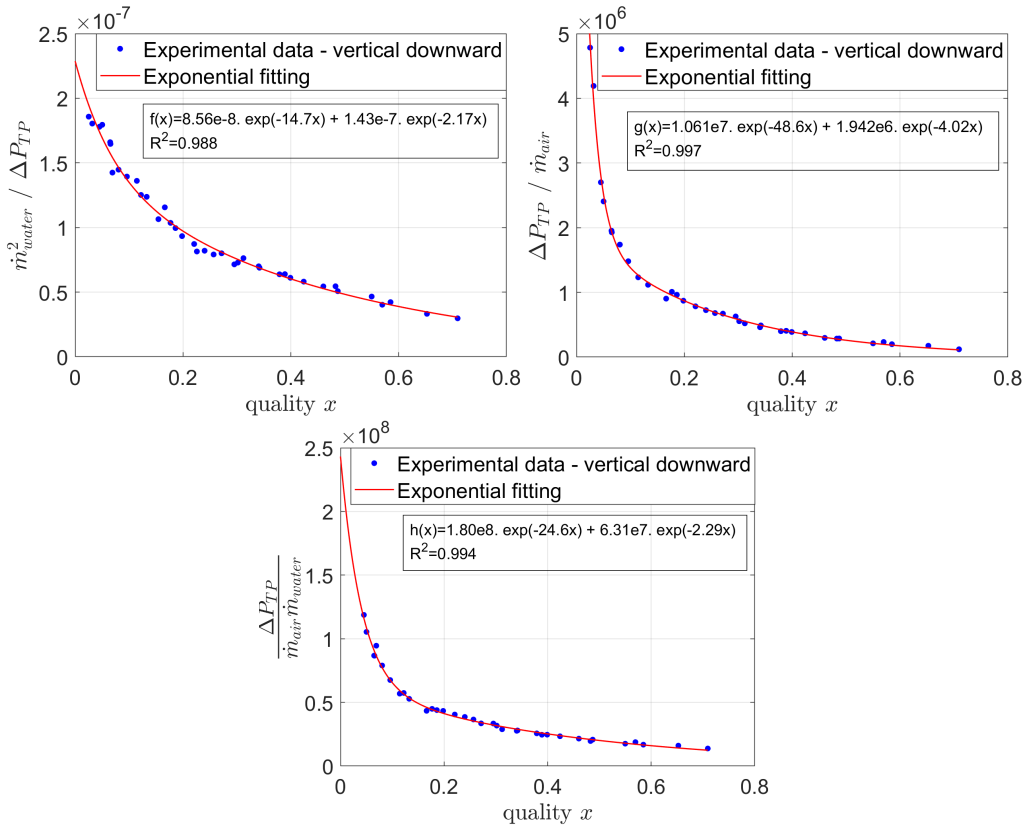

FIG. 4: Corresponding curves of Eqs. (3)–(5): experimental data and mathematical fitting equation in the vertical downward orientation solely

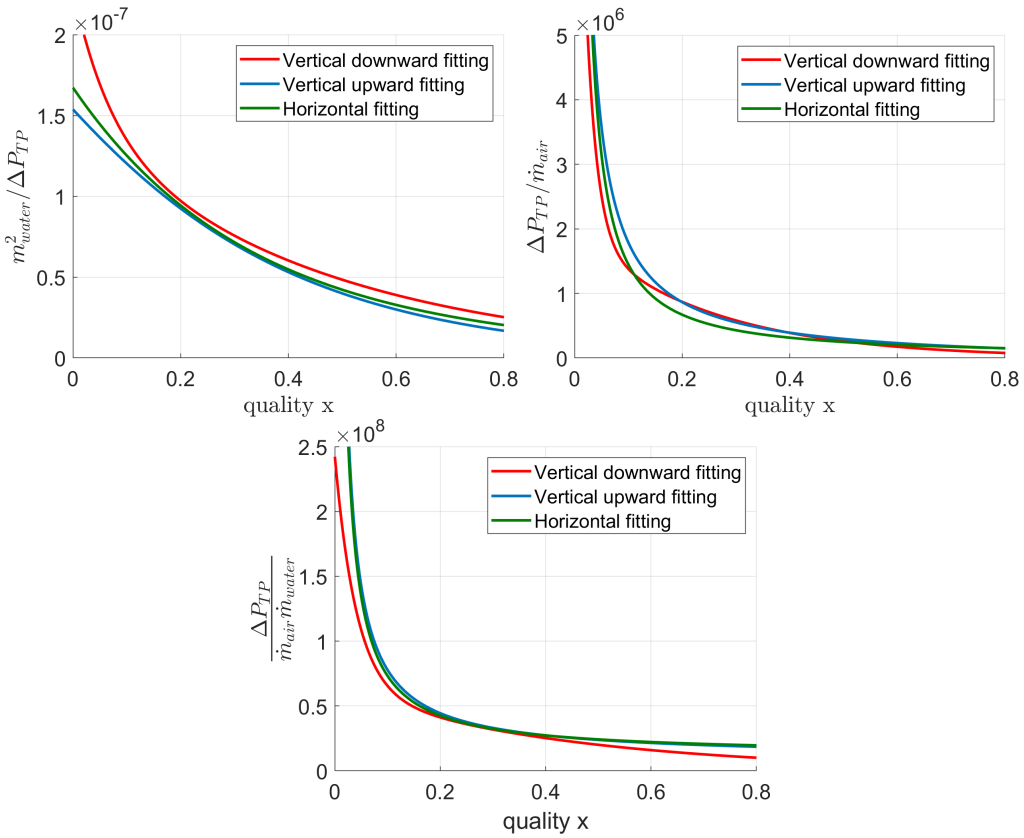

FIG. 5: Corresponding curves of Eqs. (3)–(5): mathematical fitting curves for the three orientations

Based on this set of relationships in Eqs. (3)–(5), a new approach was then developed in the present work. The schematic of the proposed methodology can be found in Fig. 6. Firstly, the VFM pressure drops signal in each channel is acquired and used as single input for the methodology. Secondly, an initial range of qualities, ranging from 0 to 1 with a step of 0.05 is selected. For each value of the quality, the respective value of the three functions $f(x)$, $g(x)$, and $h(x)$ is determined. Then the water mass flow rate $\dot{m}_{\text{water}}$ is calculated from Eq. (3) using the measured pressure drops and $f(x)$. The air mass flow $\dot{m}_{\text{air}}$ is estimated similarly using $g(x)$ and Eq. (4). The ratio $\dot{m}_{\text{air}} \times \dot{m}_{\text{water}}$ is also determined from Eq. (5) using $h(x)$. Finally, this ratio obtained from 5 is compared to the corresponding ratio $\dot{m}_{\text{air}} \times \dot{m}_{\text{water}}$ obtained from Eqs. (3) and (4), through the function $Err(x)$. When the difference of $Err(x)$ is minimal, the corresponding quality is identified. For one VFM differential pressure signal, this occurs twice, giving two possible x values. An example of the trend of $Err(x)$ is shown in Fig. 7. However, as can be seen, the two possible solutions of the quality are distant from each other. Since the quality is defined as the ratio between the vapor mass flow rate and the sum of the vapor and liquid mass flow rates, distinct quality values are thus related to different water and air mass flow rates. To be able to distinguish the appropriate x value, an analysis of the fast Fourier transform (FFT) of the VFM pressure signal is carried out. Two examples of such FFT can be seen in Figs. 8 and 9. The FFT are displayed for frequencies up to 20 Hz and not 100 Hz for the sake of clarity.

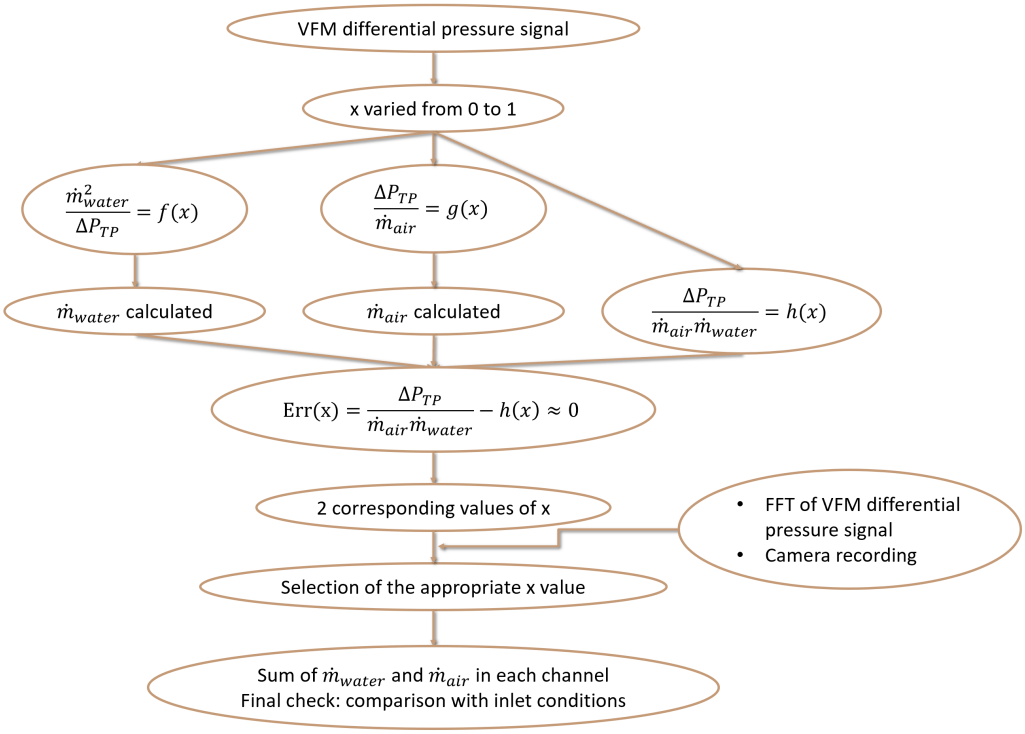

FIG. 6: Schematic of the proposed iterative methodology

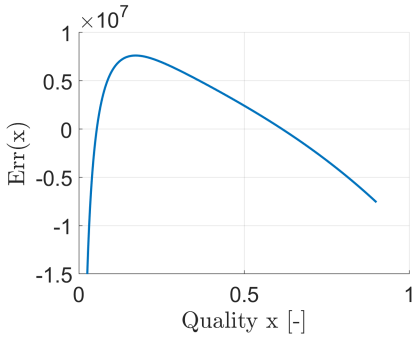

FIG. 7: Example of an $Err(x)$ curve

One can notice that the curve profile of the FFT in case of high air mass flow, and thus medium to high quality x, contains noticeable fluctuations from the frequency of 5 Hz until 15 Hz (see Fig. 8). In case of low air mass flow rate however, and thereby low quality, the curve profile is much flatter (see Fig. 9). Based on the value of the integral of the FFT curve between 5 Hz and 15 Hz and a defined threshold, the appropriate x value between the two possibilities obtained from the $Err(x)$ curve (0.05 and 0.61 in the example shown in Fig. 7) can be selected. From the chosen quality, the corresponding $\dot{m}_{\text{air}}$ and $\dot{m}_{\text{water}}$ are obtained.

The methodology displayed in the Fig. 6 is presented in the case of a single VFMs differential pressure signal input. Since there are several VFM in parallel installed on the simplified

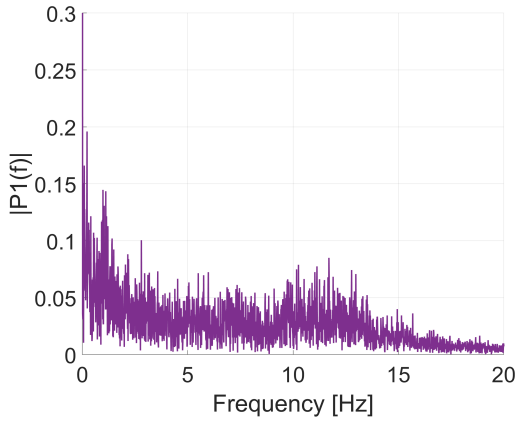

FIG. 8: Example of FFT of the VFM pressure signal in case of high air mass flow rate and low water mass flow rate

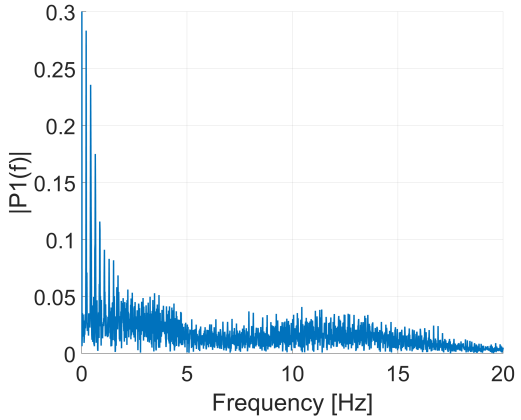

FIG. 9: Example of FFT of the VFM pressure signal in case of low air mass flow rate and medium water mass flow rate

evaporator test section (see Section 4.1), this approach has to be repeated for each VFM pressure signal from each channel. At the end of the process, the sum of the water mass flow rates in each channel is finally compared to the inlet conditions, as a final check. The same sum is performed for the air flow rates. The two-phase flow distribution inside the channels can then be obtained from these flow rates. Ultimately, a camera recording showing the two-phase flow distribution in the header can also be consulted to confirm the worthiness of the distribution.

3. UNCERTAINTIES EVALUATION AND GENERALITY OF THE METHOD

3.1 Uncertainties Evaluation

The overall uncertainty related to the experimental measurement of a quantity is calculated by considering the contribution from different sources. The measurement uncertainty of the main quantities and related to the instruments' accuracy itself has been evaluated. This information is listed in Table 1.

TABLE 1: Sensor-related uncertainties

Quantity	Uncertainty value
ΔP_{TP}	375 Pa
$\dot{m}_{\text{water,inlet}}$	0.8 g/s
$\dot{m}_{\text{air,inlet}}$	1.17 g/s

The quantification of the uncertainties related to the post-processing chain (calibration, fitting of the correlation curves, methodology...) was also achieved. To do so, the actual water and air mass flow rates as well as the quality, obtained with a single Venturi during the calibration experimental data, were compared with the estimated values from the methodology. The resulting errors are displayed in Figs. 10–12.

For the estimated quality and air mass flow, the situation is very similar. A large amount of data points are located within the $\pm$ 20% of error boundary, and almost all data points are included within the $\pm$ 30% of error. The situation is much better for the water flow rate prediction. Indeed, the majority of the estimated values do not exceed $\pm$ 10% of error, and the largest error is found to be 22%. It can also be noted that, as one could have guessed, the prediction error tends to decrease as both the water and air mass flow rates increase. Indeed, the largest errors

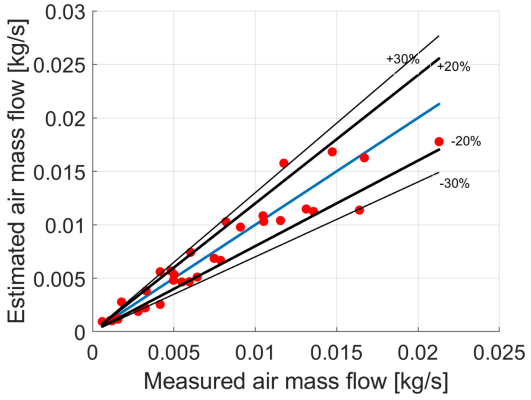

FIG. 10: Comparison between measured and estimated air mass flows

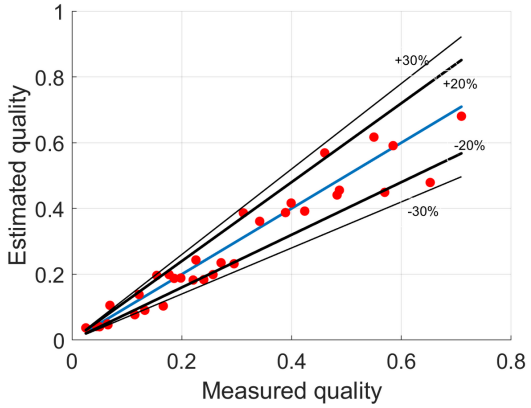

FIG. 11: Comparison between measured and estimated quality

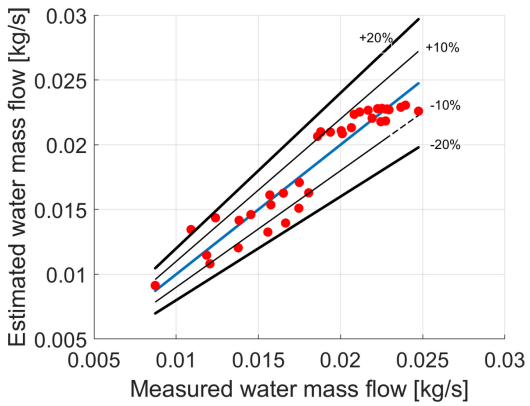

FIG. 12: Comparison between measured and estimated water mass flows

are found for the smallest mass flow rates. Since in an evaporator, the critical part relies on the distribution of the liquid phase along the channel, it is of great interest to be able to predict as accurately as possible the water mass flow rates.

3.2 Generality of the Method

The left side of the set of Eqs. (3)–(5) could be implemented for any VFM *a priori*, but the right side, meaning the mathematical fittings, are case-dependent and should be adjusted. Indeed, as one can guess, the measured two-phase pressure drops ΔP_{TP} are first greatly depending on the density of both the liquid and the gaseous phases. These pressures losses ΔP_{TP} are also impacted by the pressure test conditions as well as by the liquid and gas selected. Besides, they are also greatly influenced by the pipe diameter as well as by the throat to inlet diameter ratio β (i.e., 0.42 in this study). Thereby, the mathematical fittings $f(x)$, $g(x)$, and $h(x)$ obtained from the experimental data would have to be adapted if one of the listed parameters was modified.

Indeed, for instance, a smaller pressure test condition would greatly impact the gaseous density and volume. The gas would be lighter and its volume would increase, leading to higher pressure drops across the VFM. A larger pressure would lead to the opposite impact. A smaller pipe diameter or a smaller throat to inlet diameter ratio β would also remarkably increase the two-phase pressure drops ΔP_{TP}. This would shift the curves of the experimental data displayed in Fig. 4. Hence, the mathematical fittings presented in Fig. 5 would have to be adjusted to the new experimental data set. Attention also has to be paid to the length of the small tubes connecting the pressure taps, located at the throat and at the inlet of the VFM, and the pressure membrane sensor (see Section 2.2). These small tubes were filled with water at the beginning of each test. However, as a test runs, a fraction of this volume of water is removed and replaced by a volume of air. Since the measurement of the pressure drop depends on the value of this water column, the length of the small tubes has to be as small as possible to limit this possible source of error. As mentioned in Section 1, the great advantage of the proposed methodology is that it relies on VFM solely, without the help of any other instrument as it is commonly the case in the literature. Besides, as shown in Figs. 10–12, the errors related to this methodology are relatively low especially for the liquid phase, making it a reliable two-phase flow measurement technique. However, it requires beforehand the acquisition of a strong experimental data set as calibration, in order to obtain the trend of Eqs. (3)–(5).

4. EXPERIMENTAL APPLICATION: RESULTS AND DISCUSSION

4.1 Experimental Setup

The developed measurement methodology was applied to a simplified geometry representing an evaporator header and eight parallel channels of 10-mm I.D. An air/water mixture is used and generated with the same facility as detailed in Section 2.2. The facility is isothermal, as it was shown previously that heat transfer phenomena can be neglected in an evaporator header (Vist and Pettersen, 2004). The new methodology proposed in Section 2.3 was applied to each of the eight parallel channels to obtain their individual air and water mass flow rates. The distribution profile inside the header among the 8 channels can then be retrieved. The simplified evaporator test section (see Fig. 13) consists of a rectangular header made partly of aluminum and of dimensions 130 $\times$ 186 $\times$ 560 mm. This manifold also exhibits two transparent faces to allow flow visualizations. The feeding tube is 1.5 m long to ensure the two-phase flow development at the inlet of the test section. The diameter of the feeding tube can be varied to study its impact: 56-mm I.D. (2”) or 23-mm I.D. (3/4”); as well as its position on the header: one horizontal position and three vertical positions. A visualization block made in Plexiglass is installed at the end of the feeding pipe to monitor the inlet flow patterns. Between the visualization block and the header, a removable device can be inserted. The design selected for this device was very similar to the one detailed by Ahmad et al. (2009), which consists of a slightly curved and perforated thick plate. The objective of this accessory is to provide a pressure drop and break separated flow regimes such as stratified flow, to ensure a more uniform initial diphasic distribution. This accessory was additively manufactured in resin.

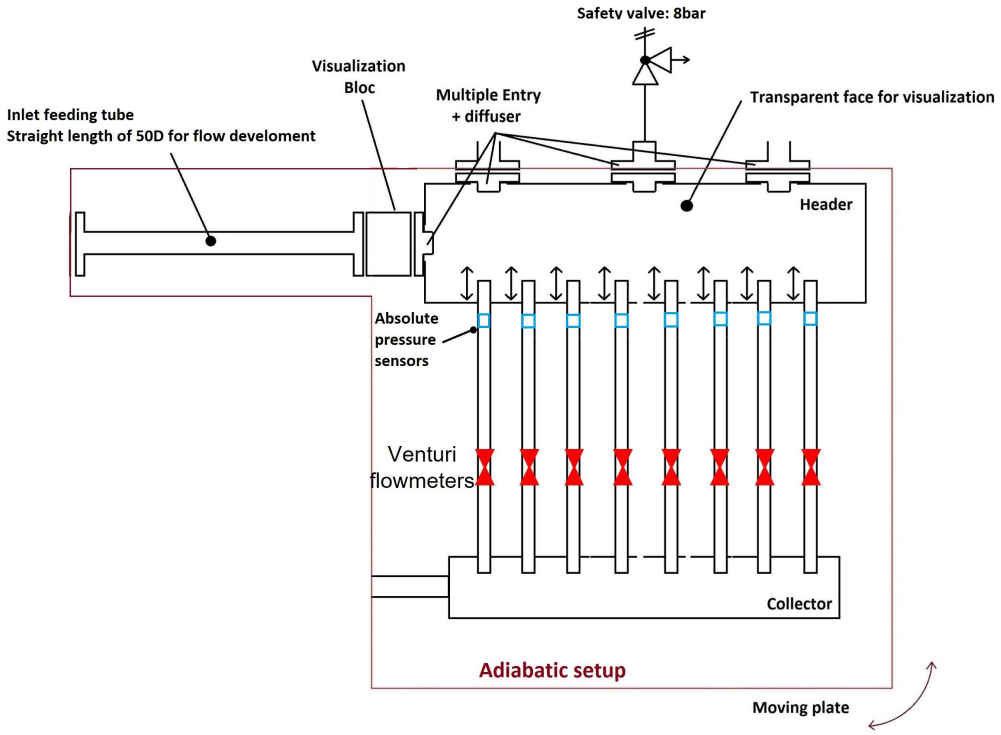

FIG. 13: Schematic of the simplified evaporator test section

A DANTEC high speed camera (SpeedSense M310) was used to record the behavior of the air/water mixture inside the header at an acquisition frequency of 500 Hz. This recording was also compared to the distribution profile obtained from the application of the methodology to the eight channels. The header is then connected to eight stainless steel channels of 10-mm I.D. The channels can be inserted inside the header, by 0, 1/4, or 1/2 of the header height, to study its influence. A VFM of same dimension as described in Section 2.2 is welded on each channel. A straight pipe length of $50D$ is installed ahead of the VFM, to ensure a developed flow. A picture of the test section can be seen on Fig. 14. Each VFM is instrumented similarly as in Section 2.2. Thus, in total, eight pressure membrane instruments were used, to obtain the throat differential pressure drop of the eight VFMs. Besides, the fluid total pressure was monitored inside the water and air inlet pipes, inside the header, and inside each of the eight channels using flush-mounted absolute pressure sensors (YA1014ABS/10V from C2AI). The fluid total temperature was monitored at the water and air inlets. A safety valve is also installed on the header to ensure that the pressure inside the test section does not exceed 8 bar. The air/water mixture is further gathered from the eight channels through a collector and then exits the test section. The orientation of this whole assembly composed of the inlet feeding tube, the header, the eight channels, and the collector can be changed. Ultimately, the purpose is to understand the impact of these combined features on the distribution of the air/water mixture inside the eight channels.

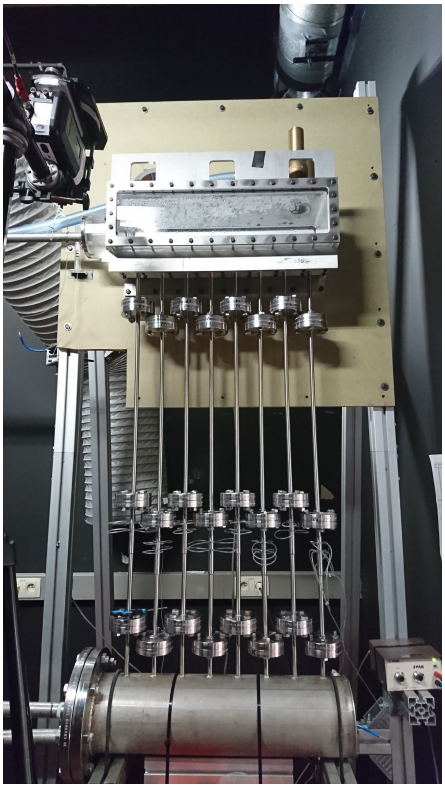

FIG. 14: Test section

4.2 Experimental Results

Thanks to the proposed methodology, the water and air mass flow rates in each channel and for each experimental point of the test matrix could be obtained. A first example of a quantitative assessment of the flow distribution can be found in Fig. 17. It shows the water mass flow rate and quality distributions among the eight channels, for a horizontal header and vertical downward channels, with a coaxial horizontal inlet of 56-mm I.D. (see Fig. 15) and no channel intrusion. The removable accessory is present. This corresponds to the configuration giving the poorest distribution that has been obtained for the configuration of a horizontal header and vertical downward oriented channels.

Indeed channel 8, which is the closest to the inlet pipe, is overfed in water by a factor 2 or 3 on average compared to the other channels (see Fig. 17). The wave created by the inlet jet when impinging the header bottom surface leads to a total avoidance of channel 6 by the water phase, to the profit of the channels located farther away. This explains the peak observable on the quality profile, meaning that the channel is mostly fed by the the air phase. The distribution profile is very similar for the channels 6, 7, and 8, whatever air and water inlet conditions are set. However, for the rest of the channels, the distribution tends to improve with the addition of water. Indeed, while the last two channels seem to be hardly reached by the water at low water inlet flow rate, the liquid phase manages to feed them properly at greater inlet conditions. Lastly, it can be noted that this largest feeding tube of 56-mm I.D. and the presence of the device fail to create an appreciable jet that would spread the liquid more uniformly inside the header. In order to improve the two-phase flow distribution in the case of a horizontal feeding tube, two possible solutions would provide similar effects: the hole diameter of the removable device and/or the feeding tube diameter should both be significantly reduced. This would greatly help in creating a more consequential jet, and thus disperse the liquid phase more evenly across the eight channels.

The second example of results that were obtained can be seen in Fig. 18. It corresponds to the combination of parameters displayed in Fig. 16: a horizontal header and vertical downward channels with a central vertical inlet of 56-mm I.D. and a channel intrusion of 1/2 of the header height. This configuration gives the most uniform distribution that could be observed for the configuration of a horizontal header and vertical downward oriented channels. It can be noted that the water feeding of all the channels is very homogeneous, and besides very stable for all applied inlet conditions. This is due to the coupling of two features: the large size of the inlet diameter that enables the smooth pouring of the water inside the header, and the channel intrusion that creates a sort of water reservoir. The water pouring interferes with its surface and generates some waves, leading to a stable and uniform feeding of all the channels. It can also be noticed through the profile of the quality, that this configuration leads to a stable air mass flow rate across the eight channels. As stated in Section 2.3, to ensure the accuracy of the water

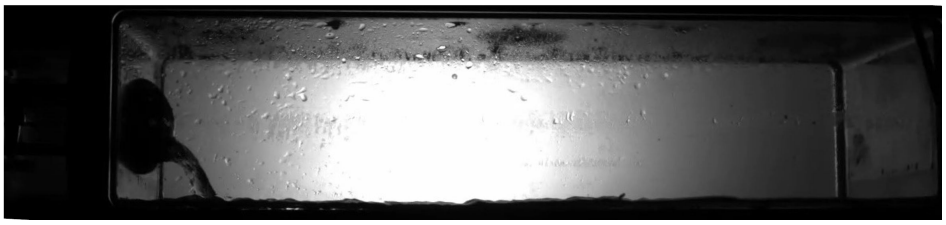

FIG. 15: Horizontal header and vertical downward channels, coaxial horizontal inlet of 56-mm I.D. and no channel intrusion

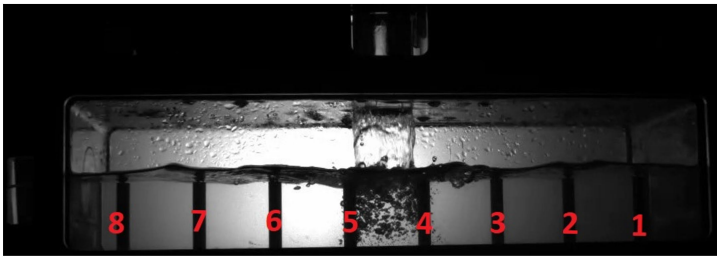

FIG. 16: Horizontal header and vertical downward channels, central vertical inlet of 56-mm I.D. and a channel intrusion of 1/2 of the header height

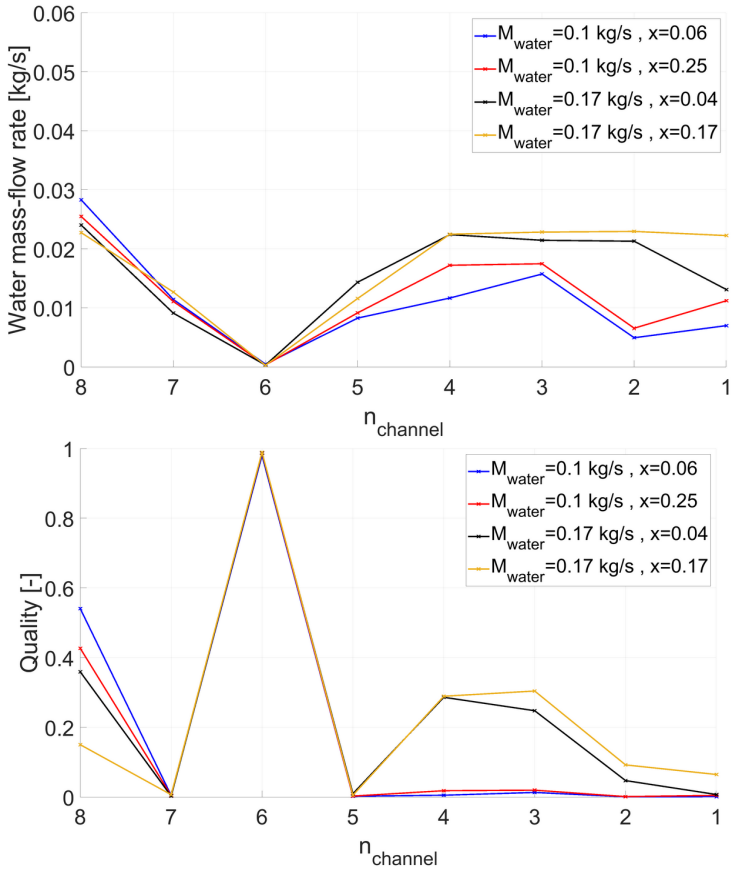

FIG. 17: Water flow rate and quality distributions corresponding to the configuration of Fig. 15, for different air and water inlet conditions

distribution profiles obtained in Figs. 17 and 18, the sum of the water mass flow rates in each of the eight channels was compared to the inlet water mass flow rate condition. The error percentage between these two values is shown in Fig. 19. The maximum error is found to be worth 35%. Consistently to what has been stated in Section 3, almost all of the error values lie within the $\pm$ 20% range, and three test points present error values around 0%.

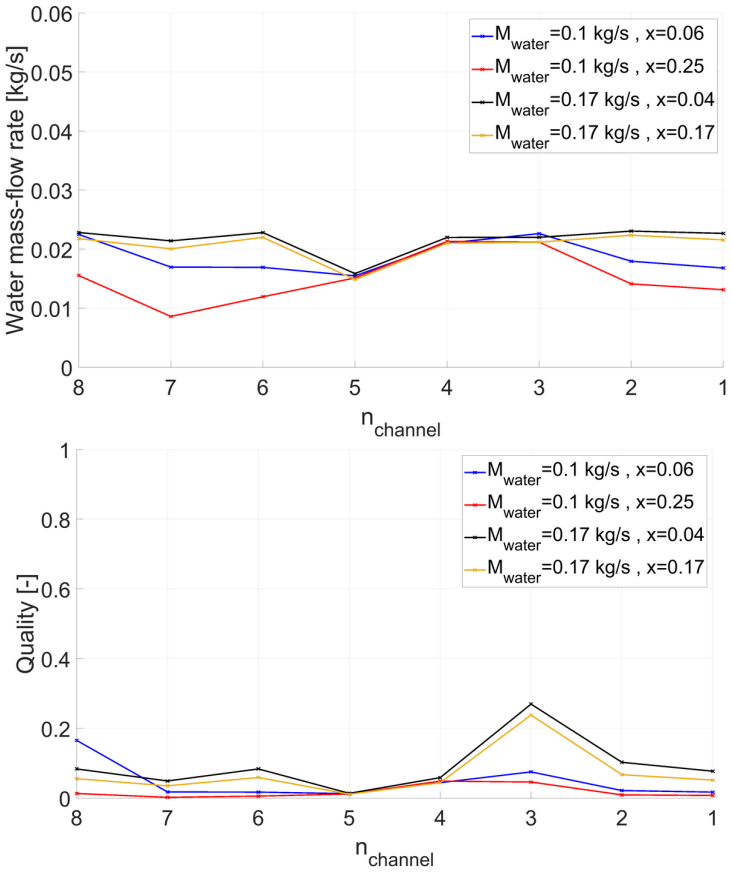

FIG. 18: Water flow rate and quality distributions corresponding to the configuration of Fig. 16, for different air and water inlet conditions

Given the rather low uncertainties obtained with the calibration tests performed on the dedicated line (see Fig. 12), and the uncertainties obtained with the actual application tests (see Fig. 19), the new proposed methodology proves to be reliable.

5. CONCLUSIONS

VFM represent a promising, inline, compact, and easy to build solution to the measurement of liquid/gas two-phase flows. They are very often found in the literature coupled with capacitance probes. However, the latter are not easily available and their design is rather dependent on the experimental conditions. Thus, the proposed methodology only based on the Venturi throat pressure drops measurement is of great necessity. Its objective is to retrieve the gas and liquid flow rates, making use of three ratios and a strong calibration prior to the tests. VFM has been applied to measure the flow distribution in a simplified isothermal evaporator header. This simplified geometry consists of a rectangular header connected to eight channels. Various parameters of this setup such as the feeding tube inlet diameter and position or the channel intrusion can be modified to understand their influence. The technique successfully managed to determine the

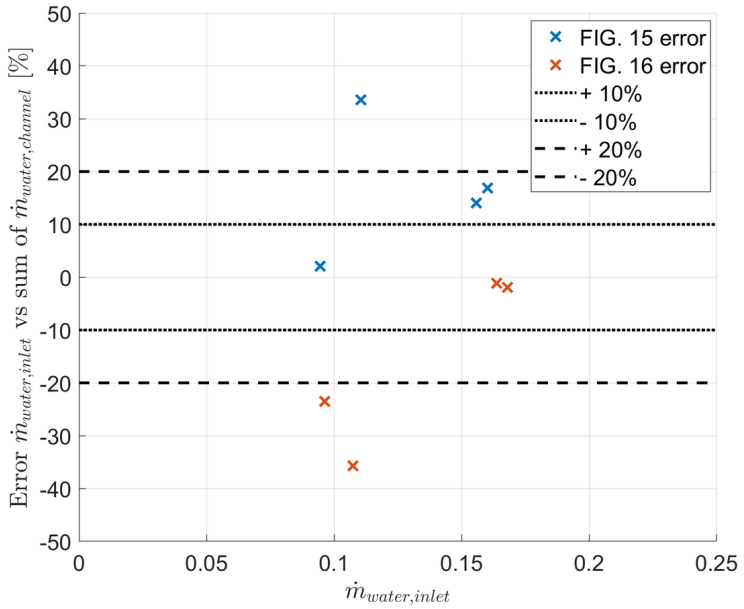

FIG. 19: Error between the inlet water mass flow rate and the sum of the individual water flow rates in each channel, for the test conditions of Figs. 17 and 18

air and water flow rates in all channels. This measurement, coupled with flow visualization in the header, enables us to draw conclusions on the effect of geometrical parameters in the flow distribution. Very different profiles of air and water flow rate feeding inside the eight channels could be obtained. Examples of a poor distribution and a uniform one have been given. In a future work, the combined effect of the header and channel orientations, channel intrusion, feeding tube position and diameter, and finally the presence or not of the removable device will be assessed using a test matrix generated thanks to a design of experiment algorithm.

ACKNOWLEDGMENTS

This work has been performed in the framework of the PANTTHER Project. This project has received funding from the Clean Sky2 Joint Undertaking (JU) (Grant Agreement No. 886698). The JU receives support from the European Union's Horizon 2020 Research and Innovation Program and the Clean Sky 2 JU members other than the Union.

REFERENCES

Ahmad, M., Berthoud, G., and Mercier, P., General Characteristics of Two-Phase Flow Distribution in a Compact Heat Exchanger, *Int. J. Heat Mass Transf.*, vol. **52**, nos. 1-2, pp. 442–450, 2009.

Baker, R.C., *Flow Measurement Handbook*, Vol. 99, Cambridge, UK: University Press Cambridge, 2000.

Bertani, C., De Salve, M., Malandrone, M., Monni, G., and Panella, B., State-Of-Art and Selection of Techniques in Multiphase Flow Measurement, Report RdS/2010/67, Torino, 2010.

Choi, J.M., Payne, W.V., and Domanski, P.A., Effects of Non-Uniform Refrigerant and Air Flow Distributions on Finned-Tube Evaporator Performance, in *Int. Congress of Refrigeration*, Washington, DC, pp. 1–8, 2003.

Dario, E.R., Tadrist, L., and Passos, J.C., Review on Two-Phase Flow Distribution in Parallel Channels with Macro and Micro Hydraulic Diameters: Main Results, Analyses, Trends, *Appl. Therm. Eng.*, vol. **59**, pp. 316–335, 2013.

de Paula Pellegrini, S., Yamaguchi, A.J., Trigo, F.C., Lima, R.G., Baliño, J.L., and Campos, S.R.V., Apparatus Design for an Independent Multiphase Flow Rate Meter, *IV Journeys in Multiphase Flows (JEM2017)*, São Paulo, Brazil, 2017.

International Organization for Standardization, Measurement of Fluid Flow by Means of Pressure Differential Devices Inserted in Circular Cross-Section Conduits Running Full, Part 4: Venturi Tubes, Standard, International Organization for Standardization, Geneva, 2003.

Leblay P., Optimisation D'un Évaporateur À Mini-Canaux Par La Maîtrise De La Distribution En Fluide Frig-Origène, PhD, Université Pierre et Marie Curie, 2012.

Lecardonnel, A., Hentorel, Y., Nour, W., Jabbour, J., Serret, D., and Laboureur, D., PANTTHER, Deliverable D1.1. Bibliographic of the Recent (Academic and Industrial) Research on VCS Evaporators, Tech. Rep., 2021.

Liu, X., Lao, L., and Falcone, G., A Comprehensive Assessment of Correlations for Two-Phase Flow through Venturi Tubes, *J. Nat. Gas Sci. Eng.*, vol. **78**, p. 103323, 2020.

Lockhart, W., Proposed Correlation of Data for Isothermal Two-Phase, Two-Component Flow in Pipes, *Chem. Eng. Prog.*, vol. **45**, no. 1, pp. 39–48, 1949.

Meng, Z., Huang, Z., Wang, B., Ji, H., Li, H., and Yan, Y., Air–Water Two-Phase Flow Measurement Using a Venturi Meter and an Electrical Resistance Tomography Sensor, *Flow Meas. Inst.*, vol. **21**, no. 3, pp. 268–276, 2010.

Monni, G., De Salve, M., and Panella, B., Two-Phase Flow Measurements at High Void Fraction by a Venturi Meter, *Prog. Nucl. Energy*, vol. **77**, pp. 167–175, 2014.

Oliveira, J.L.G., Passos, J.C., Verschaeren, R., and Van Der Geld, C., Mass Flow Rate Measurements in Gas–Liquid Flows by Means of a Venturi or Orifice Plate Coupled to a Void Fraction Sensor, *Exp. Therm. Fluid Sci.*, vol. **33**, no. 2, pp. 253–260, 2009.

Shaban, H. and Tavoularis, S., Measurement of Gas and Liquid Flow Rates in Two-Phase Pipe Flows by the Application of Machine Learning Techniques to Differential Pressure Signals, *Int. J. Multiphase Flow*, vol. **67**, pp. 106–117, 2014.

Vist, S. and Pettersen, J., Two-Phase Flow Distribution in Compact Heat Exchanger Manifolds, *Exp. Therm. Fluid Sci.*, vol. **28**, nos. 2-3, pp. 209–215, 2004.

Xie, D., Li, W., Wang, F., Zheng, J., Zheng, Y., and Liang, G., A New Method for the Flowrate Measurement of Gas–Liquid Two-Phase Flow, *IEEE Trans. Inst. Meas.*, vol. **56**, no. 4, pp. 1495–1500, 2007.

Zeghloul, A., Messilem, A., Ghendour, N., Al-Sarkhi, A., Azzi, A., and Hasan, A., Theoretical Study and Experimental Measurement of the Gas Liquid Two-Phase Flow through a Vertical Venturi Meter, *Proc. Inst. Mech. Eng. Part C: J. Mech. Eng. Sci.*, vol. **235**, no. 9, pp. 1567–1584, 2021.

Zhang, H.J., Lu, S.J., and Yu, G.Z., An Investigation of Two-Phase Flow Measurement with Orifices for Low-Quality Mixtures, *Int. J. Multiphase Flow*, vol. **18**, no. 1, pp. 149–155, 1992.